Thermodynamic Description of the ACl-ThCl4 (A = Li, Na, K) Systems

Ocadiz flores, J.A.; Rooijakkers, B.A.S.; Konings, R.; Smith, A.L.

DOI
10.3390/thermo1020009

Publication date
2021

Document Version
Final published version

Published in
Thermo

thermo

MDPI

Article

Thermodynamic Description of the ACl-$ThCl_4$ (A = Li, Na, K) Systems

Jaén A. Ocádiz Flores [1], Bas A. S. Rooijakkers [1], Rudy J. M. Konings [1,2] and Anna Louise Smith [1,*]

[1] Radiation Science & Technology Department, Faculty of Applied Sciences, Delft University of Technology, Mekelweg 15, 2629 JB Delft, The Netherlands; j.a.ocadizflores@tudelft.nl (J.A.O.-F.); b.a.s.rooijakkers@student.tudelft.nl (B.A.S.R.); r.konings@tudelft.nl (R.J.M.K.)
[2] Joint Research Centre (JRC), European Commission, Postfach 2340, D-76125 Karlsruhe, Germany
* Correspondence: a.l.smith@tudelft.nl

Abstract: The ACl-$ThCl_4$ (A = Li, Na, K) systems could be of relevance to the nuclear industry in the near future. A thermodynamic investigation of the three binary systems is presented herein. The excess Gibbs energy of the liquid solutions is described using the quasi-chemical formalism in the quadruplet approximation. The phase diagram optimisations are based on the experimental data available in the literature. The thermodynamic stability of the liquid solutions increases in the order Li < Na < K, in agreement with idealised interactions and structural models.

Keywords: thorium; thorium tetrachloride; molten salt reactor; CALPHAD; quasi-chemical formalism

Citation: Ocádiz Flores, J.A.; Rooijakkers, B.A.S.; Konings, R.J.M.; Smith, A.L. Thermodynamic Description of the ACl-$ThCl_4$ (A = Li, Na, K) Systems. *Thermo* **2021**, *1*, 122–133. https://doi.org/10.3390/thermo1020009

Academic Editor: Andrew S. Paluch

Received: 31 May 2021
Accepted: 13 July 2021
Published: 16 July 2021
Corrected: 8 November 2022

1. Introduction

Glenn Seaborg called the discovery of ^{232}Th being a fertile isotope, yielding fissile ^{233}U after neutron absorption and subsequent decay, 'a fifty quadrillion discovery' [1]. That notwithstanding, industrial use of thorium is still virtually non-existent in modern-day society. If it is to fulfill its potential as a vastly abundant energy source, reactor and fuel cycle designs are needed that are optimised for the efficient breeding and utilisation of ^{233}U. Studies have shown that thorium can be used in a wide variety of reactors [2]. Therefore it is important to continue characterizing the thermophysical properties of the chemical forms it may take as an advanced nuclear fuel, e.g., metallic, oxide, nitride, or halide. As part of that effort, a thermodynamic description of the binary systems ACl-$ThCl_4$ (A = Li, Na, K) is presented herein, since these are systems from which metallic thorium powder may be produced [3], and because they may be part of a fuel matrix in a molten salt reactor (MSR) [4]. Metal chlorides are receiving increasing attention in the MSR community, as they allow high loading of actinides compared to the more studied fluorides, although they are best suited for fast neutron systems.

Even though it has been the subject of several studies, $ThCl_4$ is not fully characterised. It has been reported to crystallise in two phases. The low-temperature phase is tetragonal in space group $I4S_1/a$, while the high-temperature phase belongs to space group $I4_1/amd$ [5]. The latter phase is metastable below the phase transition temperature, 679 K, and it is the one usually reported by experimentalists [6–11]. The low-temperature phase has only been isolated by Mason et al. [12], who used a very slow cooling rate. For this reason, the recommended thermodynamic data in the literature is for the high-temperature polymorph. The value of the standard enthalpy of formation recommended by Fuger et al. [5] is an average of values determined via solution calorimetry [13–15]. The standard entropy was estimated by Konings considering lattice and electronic contributions [16], and the high-temperature heat capacity was estimated by Rand [17]. Intriguingly, there could also be a very low-temperature phase, below 70 K [18].

Some studies for the ACl-$ThCl_4$ (A = Li, Na, K) binary phase diagrams are available in the literature. However, despite this and their apparent simplicity compared to their fluoride counterparts, their topology is not well-established. In the LiCl-$ThCl_4$ system, Oyamada found no intermediate phase [19], yet Vokhmyakov et al. [20], Tanii [21],

and Vdovenko et al. (original work not available to us, but described in *The Chemistry of Actinide and Transactinide Elements [22]*) [23] observed an incongruently melting compound of composition Li_4ThCl_8. In the NaCl-$ThCl_4$ system, all available sources agree on the existence of Na_2ThCl_6 and no other compound, but Vdovenko et al. [23] observed $NaThCl_5$ instead. Finally, in the KCl-$ThCl_4$ system, different groups report the existence of K_3ThCl_7, K_2ThCl_6, and $KThCl_5$. The observations are summarised in Table 1.

Table 1. Phases occurring in the alkali thorium chloride binary systems according to different sources.

System	Compounds	References
LiCl-$ThCl_4$	Li_4ThCl_8	[20,21,23]
	none	[19]
NaCl-$ThCl_4$	Na_2ThCl_6	[19–21]
	$NaThCl_5$	[23]
KCl-$ThCl_4$	K_3ThCl_7	[19,24]
	K_2ThCl_6	[21,24]
	$KThCl_5$	[19,24]

From these mixed accounts, it can be seen that there is a need for a comprehensive study to establish a coherent description of these phase diagrams. An interpretation of their most likely topology is put forward in this work, and CALPHAD models for their calculation are presented.

2. Thermodynamic Modelling

2.1. Pure Compounds

The thermodynamic assessments were performed with the Factsage software [25] (Version 7.2). A thermodynamic assessment consists of optimising unknown parameters related to the Gibbs energy functions of all the phases occurring in a system, in order to develop a thermodynamic model consistent with experimentally determined information such as phase diagram equilibria, thermodynamic data, enthalpies of fusion, vapour pressures, and activities. The Gibbs energy function of a pure end-member in a system is given by:

$$G^{\circ}(T) = \Delta_f H^{\circ}_{\mathrm{m}}(298) - S^{\circ}_{\mathrm{m}}(298)T + \int_{298}^{T} C^{\circ}_{\mathrm{p,m}}(T)dT - T\int_{298}^{T} \frac{C^{\circ}_{\mathrm{p,m}}(T)}{T}dT \quad (1)$$

where $\Delta_f H^{\circ}_{\mathrm{m}}(298)$ is the standard enthalpy of formation, and $S^{\circ}_{\mathrm{m}}(298)$ is the standard absolute entropy, both evaluated at a reference temperature, typically taken to be 298.15 K (denoted here as 298 K for simplicity). $C_{\mathrm{p,m}}$ is the isobaric heat capacity expressed as a polynomial:

$$C_{\mathrm{p,m}}(T) = a + bT + cT^2 + dT^{-2} \quad (2)$$

Isobaric heat capacity data is only available for the end-members. To estimate the heat capacities and standard entropies of intermediate compounds, the Neumann-Kopp rule [26] was applied.

The thermodynamic functions of LiCl(cr,l) and KCl(cr,l) were taken from the SGPS [27]. Those of NaCl(cr,l) were taken from the IVTAN tables by Glushko et al. [28], while the heat capacity of NaCl(l) was recently recommended by van Oudenaren et al. [29]. The authors critically reviewed the four studies available on the determination of the heat capacity of NaCl(l) [30–33] and found that there was no discrepancy between the data by Dawson et al. [33] and the rest of the authors, in contrast with what Glushko et al. had argued. Considering the average of the four studies, van Oudenaren et al. recommend (68 ± 1) kJ $\cdot$ mol^{-1} in the 1074 to 2500 K range. In the case of $ThCl_4$(cr,l), the data used were recommended by Fuger et al. [5] and Capelli and Konings [34]. As mentioned in the introduction, $ThCl_4$ crystallises in two phases. Using an adiabatic calorimeter, Chiotti et al. [35] measured an enthalpy of transition equal to (5.0 ± 1.5) kJ $\cdot$ mol^{-1} at (679 ± 2) K. Taking

the heat capacity of $ThCl_4$-α (the low-temperature phase) to be equal to that recommended for $ThCl_4$-β (the high-temperature phase), the standard enthalpy of formation and standard entropy of $ThCl_4$-α were optimised in this work, such that the transition between both phases matched the values reported by Chiotti et al. [35]. The enthalpy of fusion (61.5 $\pm$ 5.0) kJ $\cdot$ mol^{-1}, melting temperature (T = 1042 K), and heat capacity recommended by Capelli and Konings [34] were used to describe $ThCl_4$(l). The thermodynamic functions of the intermediate compounds were optimised in this work to match the experimentally determined phase diagrams as closely as possible. All values are given in Table 2.

Table 2. Thermodynamic data for intermediate compounds used in this work for the phase diagram assessment: $\Delta_f H^o_m$(298 K)/(kJ ·mol^{-1}), S^o_m(298 K)/(J·K^{-1}·mol^{-1}), and heat capacity coefficients $C_{p,m}$(T/K)/(J·K^{-1}·mol^{-1}), where $C_{p,m}(T/K) = a + b\cdot T + c\cdot T^2 + d\cdot T^{-2} + e\cdot T^3$. Optimised data are shown in **bold**.

Compound	$\Delta_f H^o_m$(298 K)/(kJ·mol^{-1})	S^o_m(298 K)/(J·K^{-1}·mol^{-1})	$C_{p,m}$(T/K)/(J·K^{-1}·mol^{-1}) = a + b·T + c·T^2 + d·T^{-2}				Range	Reference
			a	b	c	d		
LiCl(cr)	−408.266	59.3	44.70478	0.01792765	1.863482×10^{-6}	−194,457.7	298–883	[27]
			73.30619	−0.009430108		33,070.5	883–2000	[27]
LiCl(l)	−388.4342	81.76	44.70478	0.01792765	1.863482×10^{-6}	−194,457.7	298–883	[27]
			73.30619	−0.009430108		33,070.5	883–2000	[27]
NaCl(cr)	−411.260	72.15	47.72158	0.0057	1.21466×10^{-5}	−882.996	298–1074	[28]
NaCl(l)	−390.853	83.302	68.0				298–2500	[28,29]
KCl(cr)	−436.6841	82.555	50.47661	0.005924377	7.496682×10^{-6}	−144,173.9	298–700	[27]
			143.5698	−0.1680399	9.965702×10^{-5}	−8,217,836	700–1044	[27]
			73.59656			−8,217,836	1044–2000	[27]
KCl(l)	−410.4002	107.7311	50.47661	0.005924377	7.496682×10^{-6}	−144,173.9	298–700	[27]
			143.5698	−0.1680399	9.965702×10^{-5}	−8,217,836	700–1044	[27]
			73.59656				1044–2000	[27]
α-$ThCl_4$(cr)	**−1191.3012**	**176.135**	120.293	0.0232672		−615,050	298–1042	this work, [35]
β-$ThCl_4$(cr)	−1186.300	183.499	120.293	0.0232672		−615,050	298–1042	[5,34]
$ThCl_4$(l)	−1149.740	197.626	167.4				298–1500	[5,34]
Li_4ThCl_8(cr)	**−2834.966**	**413.34**	299.11212	0.0949778	7.453928×10^{-6}	−1,392,880.8	298–883	this work
			413.51776	−0.014453232		−482,768	883–1042	
			437.1957	−0.037720432		132,282	1042–2000	
Na_2ThCl_6(cr)	**−2051.540**	**328.0**	215.73616	0.0346672	2.42932×10^{-5}	−616,815.992	298–1042	this work
			239.41	0.0114	2.42932×10^{-5}	−1765.992	1042–1074	
$KThCl_5$(cr)	**−1685.000**	**258.69**	170.76961	0.029191577	7.496682×10^{-6}	−759,223.9	298–700	this work
			263.8628	−0.1447727	9.965702×10^{-5}	−8,832,886	700–1042	
			287.5408	−0.1680399	9.965702×10^{-5}	−8,217,836	1042–1044	
			217.568				1044–2000	
K_2ThCl_6(cr)	**−2139.850**	**380.5**	221.24622	0.035115954	1.4993364×10^{-5}	−903,397.8	298–700	this work
			407.4326	−0.3128126	1.9931404×10^{-4}	−17,050,722	700–1042	
			431.1106	−0.3360798	1.9931404×10^{-4}	−16,435,672	1042–1044	
			291.16408				1042–2000	

2.2. Liquid Solution

The excess Gibbs energy terms of liquid solutions were modelled using the modified quasi-chemical model in the quadruplet approximation proposed by Pelton et al. [36]. This formalism is apt to describe ionic liquids like the melts examined here, as it allows to select the composition of maximum short-range ordering (SRO) by varying the ratio between the cation-cation coordination numbers $Z^A_{AB/Cl}$ and $Z^B_{AB/Cl}$ (see Table 3). It has been used to assess a significant number of molten salt systems for nuclear applications [37,38], becoming a standard of sorts for the MSR thermochemistry community [39]. Despite its practicality, structural features, such as molecular species and network formation, are not accounted for. However, structural features may be imposed on the model, for example by explicitly introducing ions with different coordinations [40,41]. In this formalism, a set of two anions and two cations makes up a quadruplet, taken to be the basic unit in the liquid solution, and the excess parameters to be optimised are those related to the following second-nearest neighbour (SNN) exchange reaction:

$$(A - Cl - A) + (B - Cl - B) \longrightarrow 2(A - Cl - B) \quad \Delta g_{AB/Cl} \tag{3}$$

where the chloride anions are represented by Cl, and A and B denote the cations. $\Delta g_{AB/Cl}$ denotes the Gibbs energy change associated with the SNN exchange reaction:

$$\Delta g_{AB/Cl} = \Delta g^{0}_{AB/Cl} + \sum_{i \geqslant 1} g^{i0}_{AB/Cl} \chi^{i}_{AB/Cl} + \sum_{j \geqslant 1} g^{0j}_{AB/Cl} \chi^{j}_{BA/Cl} \quad (4)$$

$\Delta g^{0}_{AB/Cl}$ and $g^{ij}_{AB/Cl}$ are coefficients which may have temperature dependence, but which are independent of composition. The composition dependence is specified by the $\chi_{AB/Cl}$:

$$\chi_{AB/Cl} = \frac{X_{AA}}{X_{AA} + X_{AB} + X_{BB}} \quad (5)$$

where X_{AA}, X_{BB} and X_{AB} represent cation-cation pair mole fractions. Finally, charge conservation over the quadruplet imposes the anion coordination number:

$$\frac{q_A}{Z^{A}_{AB/Cl}} + \frac{q_B}{Z^{B}_{AB/Cl}} = \frac{2q_{Cl}}{Z^{Cl}_{AB/Cl}} \quad (6)$$

where q_i are the charges of the different ions, and $Z^{Cl}_{AB/Cl}$ is the anion-anion coordination number. These were chosen to represent the composition of maximum short-range ordering, where the Gibbs energy tends to have its minimum. Typically, the point of maximum short-range ordering can be expected to lie near the lowest eutectic. The cation-cation coordination numbers are listed in Table 3.

Table 3. Cation-cation coordination numbers of the liquid solution.

A	B	$Z^{A}_{AB/Cl}$	$Z^{B}_{AB/Cl}$
Li^+	Li^+	6	6
Na^+	Na^+	6	6
K^+	K^+	6	6
Th^{4+}	Th^{4+}	6	6
Li^+	Th^{4+}	4	6
Na^+	Th^{4+}	3	6
K^+	Th^{4+}	4	6

The optimised excess Gibbs energy parameters of the binary liquid solutions are shown in Equations (7)–(9). The parameters were optimised based on the phase diagram equilibria points of the liquidus.

$$\Delta g_{LiTh/Cl} = -8000 - 3600 \cdot \chi_{LiTh/Cl} - 7300 \cdot \chi_{ThLi/Cl} \text{ J} \cdot \text{ mol}^{-1} \quad (7)$$

$$\Delta g_{NaTh/Cl} = -27,700 - 7500 \cdot \chi_{NaTh/Cl} - 14,000 \cdot \chi_{ThNa/Cl} \text{ J} \cdot \text{ mol}^{-1} \quad (8)$$

$$\Delta g_{KTh/Cl} = -40,000 - 10,000 \cdot \chi_{ThK/Cl} \text{ J} \cdot \text{ mol}^{-1} \quad (9)$$

3. Results and Discussion

3.1. Phase Diagrams

The calculated phase diagrams are shown in Figures 1–3, and invariant equilibria are listed in Table 4. For the LiCl-$ThCl_4$ system, the modelling choice to include Li_4ThCl_8 was very clear: three different authors reported they had observed it. Incidentally, in the LiCl-UCl_4 phase diagram there is also a ternary chloride, although the formula is Li_2UCl_6 [42]. It has been determined to belong to space group $P6_3/mmc$ [43]. The calculated phase diagram closely reproduces the equilibria found by Tanii [21]. The melting points of the end-members measured by Tanii agree well with the recommended values, indicating quite pure reagents. Oyamada [19], on the other hand, reports melting points for the

end-members which are more than 20 K higher, which could be due to oxygen or water contamination. It can be seen that the $\alpha - \beta$ transition of $ThCl_4$ is very close to the eutectic of the system, which would make both events very difficult to resolve experimentally.

In the NaCl-$ThCl_4$ system, the modelling choice is also clear: three authors agree that Na_2ThCl_6 forms and that is melts congruently, and only Vdovenko et al. [23] report a different stoichiometry ($NaThCl_5$). In the analogous NaCl-UCl_4 system a compound with formula $NaUCl_5$ was not observed, but Na_2UCl_6 was [42,44,45]. Furthermore, its crystal structure was studied and it is known to belong to space group *P-3m1* [43]. These observations support the choice to include Na_2ThCl_6. In this phase diagram the $\alpha - \beta$ transition of $ThCl_4$ is again very close to the second eutectic of the system, making it experimentally difficult to observe.

The KCl-$ThCl_4$ system has greatest discrepancies in the $0.25 < ThCl_4 < 0.33$ region. Gershanovich and Suglobova [24] reported both K_3ThCl_7 and K_2ThCl_6, Oyamada [19] reported only the former, and Tanii [21] and Vokhmyakov [20] reported only the latter (see Table 1). In fact, Gershanovich and Suglobova [24] characterised the crystal structure of K_2ThCl_6, which belongs to space group *Cmcm*, so this phase was retained in the assessment. Including K_3ThCl_7 raises the liquidus around the line compound and can be done without re-optimising the Gibbs energy terms of the other intermediate phases. However, much larger excess Gibbs energy parameters would need to be imposed on the liquid solution to obtain in this new optimisation the solidus temperature close to the experimental points. Relying, yet again, on what is known on the KCl-UCl_4 system, in which a phase with formula K_2UCl_6 was reported [42,44], the phase K_3ThCl_7 was discarded. As for $KThCl_5$, Tanii [21] is the only author who did not suggest its existence, although his calorimetric measurements form a concavity with a maximum centered around $X(ThCl_4) = 0.5$ (Figure 3, ⁎), which can very well be interpreted as the congruent melting of a phase with stoichiometry $KThCl_5$. For that reason, the phase was retained in the assessment.

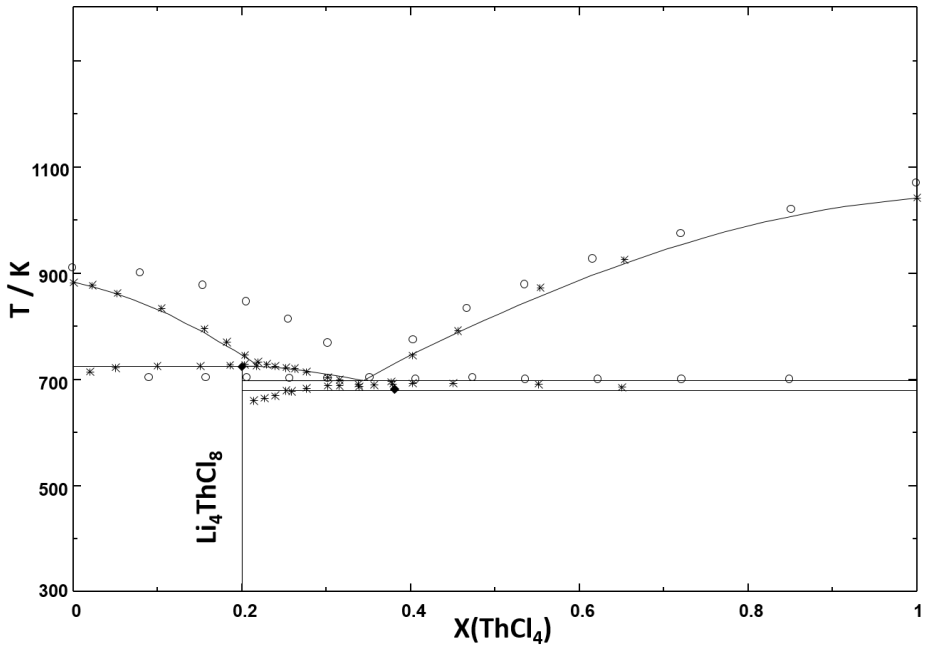

Figure 1. The LiCl-$ThCl_4$ phase diagram as calculated in this work. Symbols: phase diagram data reported by Tanii [21] (⁎), Oyamada [19] (○), and Vokhmyakov et al. [20] (⬥).

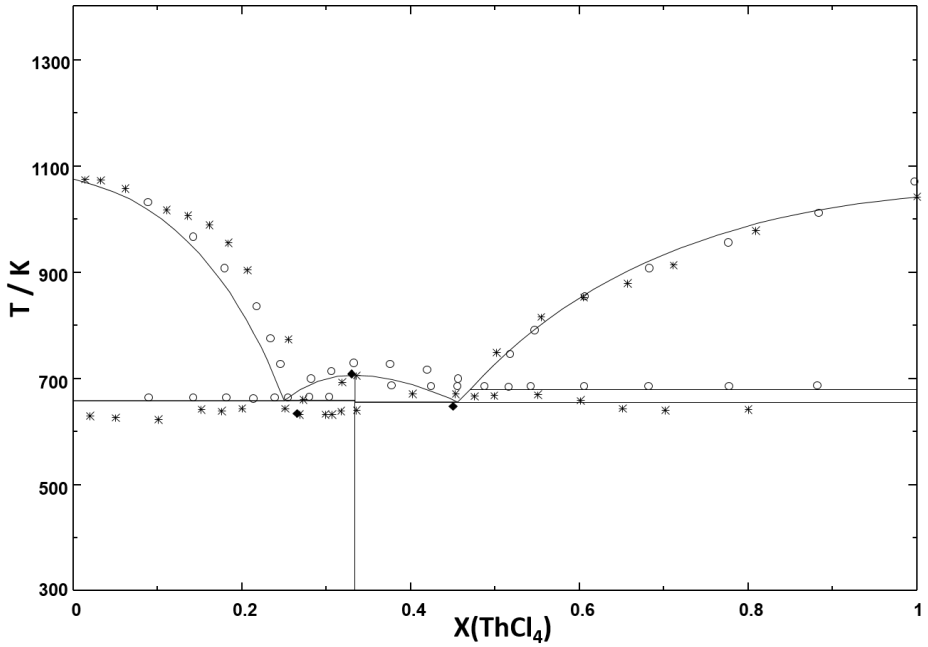

Figure 2. The NaCl-$ThCl_4$ phase diagram as calculated in this work. Symbols: phase diagram data reported by Tanii [21] (⁎), Oyamada [19] (○), and Vokhmyakov et al. [20] (♦).

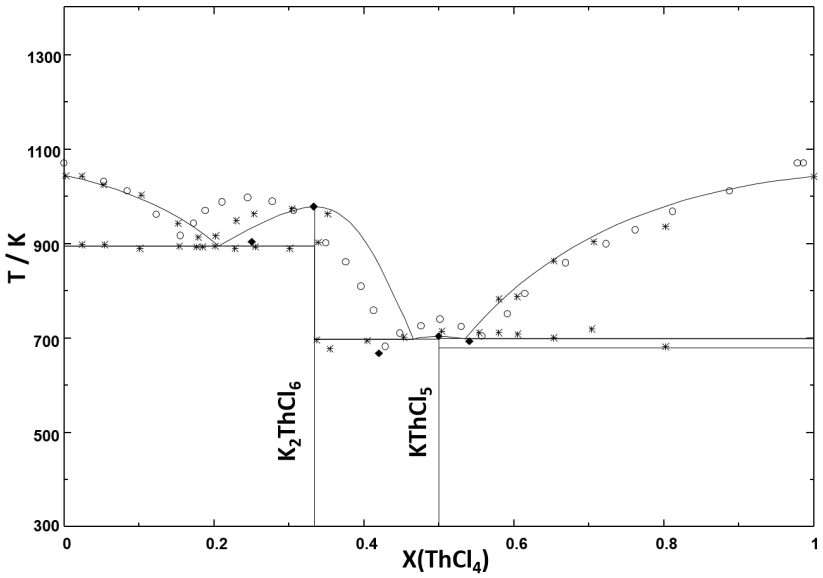

Figure 3. The KCl-$ThCl_4$ phase diagram as calculated in this work. Symbols: phase diagram data reported by Tanii [21] (⁎), Oyamada [19] (○), and Vokhmyakov et al. [20] (♦).

Table 4. Invariant equilibrium data in the ACl-$ThCl_4$ systems.

System	Equilibrium	Invariant Reaction	This Study (calc.)		Tanii et al. [21]		Vokhmyakov et al. [19]		Oyamada [20]	
			X($ThCl_4$)	T / K	X($ThCl_4$)	T / K	X($ThCl_4$)	T / K	X($ThCl_4$)	T / K
LiCl-$ThCl_4$	Congruent Melting	LiCl = L	1	883	1	881			1	910
	Peritectic	Li_4ThCl_8 = LiCl + L	0.2	723	0.2	725	0.2	723	-	-
	Eutectic	Li_4ThCl_8 + β-$ThCl_4$ = L	0.343	695	-	690	0.38	681	0.35	703
	α-β transition	α-$ThCl_4$ = β-$ThCl_4$	1	679						
	Congruent Melting	β-$ThCl_4$ = L	1	1042	1	1041			1	1070
NaCl-$ThCl_4$	Congruent melting	NaCl = L	0	1074	0	1074			0	1097
	Eutectic	NaCl + Na_2ThCl_6 = L	0.251	657	-	639	0.255	633	0.26	667
	Congruent Melting	Na_2ThCl_6 = L	1/3	703	1/3	708	1/3	708	1/3	729
	Eutectic	Na_2ThCl_6 + α-$ThCl_4$ = L	0.457	654	-	637	0.45	648	0.49	686
KCl-$ThCl_4$	Congruent melting	KCl = L	0	1044	0	1043			0	1070
	Eutectic	KCl + K_2ThCl_6 = L	0.206	894	-	895	0.25	903	0.15	917
	Congruent melting	K_2ThCl_6 = L	1/3	977	1/3	988	1/3	978	0.25 [a]	997
	Eutectic	K_2ThCl_6 + $KThCl_5$ = L	0.467	697	-	705	0.42	668	0.43	681
	Congruent melting	$KThCl_5$ = L	0.5	702			0.5	703	0.5	741
	Eutectic	$KThCl_5$ + β-$ThCl_4$ = L	0.536	699			0.54	693	0.56	706

[a] Interpreted by the author to be the congruent melting of K_3ThCl_7.

3.2. Enthalpy of Mixing

The mixing enthalpies are of great interest since they are linked to the stability of the liquid solutions. They have not been measured for these systems, yet the calculated values, shown in Figure 4a (T = 1100 K), may serve as another dataset, apart from the phase diagrams, to gauge the validity of the models optimised here. There are three things to notice. First of all, the mixing enthalpies are negative at all compositions. Second, the depth of the curves increases in magnitude in the order Li < Na < K. Third, the curves are not symmetric, but display minima in the ACl-rich regions (A = Li, Na, K). Although ions do not behave like hard charged spheres [46], it may be a useful exercise to model them with such an idealised potential in order to gain insight into the energetics of mixing in the melt:

$$V_{qq}(r_{ij}) = \sum_{i<j} \frac{q_i q_j}{r_{ij}} \quad r_{ij} > r_{0,ij} \tag{10}$$

$$V_{rep}(r_{ij}) = \infty \quad r_{ij} \leqslant r_{0,ij} \tag{11}$$

In Equations (10) and (11), q denotes formal charge of ions i and j , r_{ij} is the internuclear distance, and $r_{0,ij}$ is the sum of the radii of ions i and j. Retaining the quadruplets as a crude structural model, the energy change upon SNN exchange (Equation (3)) is:

$$\Delta V_{SNNexchange} = 2\frac{q_A q_{Th} + q_{Cl} q_{Cl}}{\sqrt{r_{ThCl}^2 + r_{ACl}^2}} - \frac{q_{Th} q_{Th} + q_{Cl} q_{Cl}}{r_{ThCl}\sqrt{2}} - \frac{q_A q_A + q_{Cl} q_{Cl}}{r_{ACl}\sqrt{2}} \tag{12}$$

In rocksalt structures, the cation-anion coordination number is 6, and a coordination number of 6 has been seen to be prevalent about Th^{4+} in LiCl-$ThCl_4$ melts with molecular dynamics (MD) simulations [47]. Taking into account the Shannon radii [48] for such coordinations, the values in Table 5 are obtained. Note that they are meant only to illustrate general qualitative trends: a quantitative description requires taking into account physically realistic structural models and multiple interactions over the long range, as in molecular dynamics simulations.

Table 5. Change in exchange energy due to SNN exchange reactions.

Ion	Coordination [a]	Shannon Ionic Radius r_i(Å) [48]	$\Delta V_{SNNexchange}$ (Hartree)
Li^+	VI	0.76	−4.1
Na^+	VI	1.0	−4.2
K^+	VI	1.38	−4.9
Th^{4+}	VI	0.94	
Cl^-	VI	1.81	

[a] Not to be confused with the cation-cation coordination number of Table 3.

From this simplified picture, the enthalpies of mixing can be expected to be favourable from a Coulombic point of view. Moreover, Table 5 agrees with the trend of progressive stabilisation with increasing alkali radius shown by the curves in Figure 4(**a**). This trend is also related to an increased stability of first-nearest neighbour (FNN) shells around Th^{4+} as the polarizing ability of the alkali cation diminishes with increasing size [49]. Furthermore, if the mixing event is considered as an acid-base reaction:

$$nACl + ThCl_4 = [ThCl_{4+n}]^{-n} + nA^+ \quad (13)$$

the increasing radius of the alkali cation implies its charge is spread over a larger volume, resulting in a more stable conjugate chloroacid A^+, contributing to the overall stability of the liquid solution. The third effect, the asymmetry, is related to the choice of cation-cation coordination numbers (Table 3), chosen to reflect the compositions of the lowest-melting eutectics and maximum short-range ordering. Such an asymmetry would also be expected in experimentally measured curves. For instance, calorimetric studies of the ACl-MCl_2 systems (M = Mn, Fe, Co, Ni, Cd; A = Li, Na, K, Rb, Cs) [50–52] revealed a minimum for the enthalpy of mixing near X(MCl_2)=0.33, the stoichiometry which favours the formation of tetrahedral MCl_4^{2-} complexes in the melt. Complexes of these kind have been observed spectroscopically in studies in which $NiCl_2$ is dissolved in alkali chlorides [53,54]. The coordination of $[ThCl_x]^{4-x}$ shells has been studied with Raman spectroscopy by Photiadis and Papatheodorou [55], and they were found to be 6 (octahedral) and 7-coordinated (pentagonal bipyramidal) in melts rich in alkali chloride (A = Li, Na, K, Cs). Beyond ∼0.3 $ThCl_4$ content, bridging of these shells was observed via shared chlorides, up to pure $ThCl_4$. The relatively limited stability of $(ThCl_x)^{4-x}$ cages when LiCl is the solvent, compared to the other alkali chlorides would yield the most symmetric curve, as in Figure 4a. Calorimetric measurements have shown this to be the case for the (Li,Th)F_x melt [56].

The thermodynamic stability of solutions is also affected by entropy effects. For example, in systems with shallow mixing enthalpies and negative mixing entropies, miscibility gaps may result, although that is more common in metallic systems [57]. In the present systems, the calculated mixing entropies of the (Li,Th)Cl_x and (Na,Th)Cl_x liquid solutions are positive throughout the composition range (Figure 4b), contributing to the stability of the mixtures. In agreement with the structural features just discussed, (Li,Th)Cl_x tends to regular solution behaviour, and (Na,Th)Cl_x deviates from regularity, showing a minimum at the point of maximum short-range ordering (SRO). (K,Th)Cl_x displays such strong SRO that the entropy of mixing approaches zero at its minimum near X($ThCl_4$) = 0.4: the mixing is least favourable from an entropic perspective where it is most favourable from an enthalpic point of view. However, the mixing enthalpies dominate the contribution, and the Gibbs energies of mixing which govern overall liquid phase stability are arranged in the same order (Figure 5). A high stability of the liquids is a desirable property, as it makes it more likely to find alloys which can withstand their corrosive properties, as well as contributing to their stability under irradiation [58].

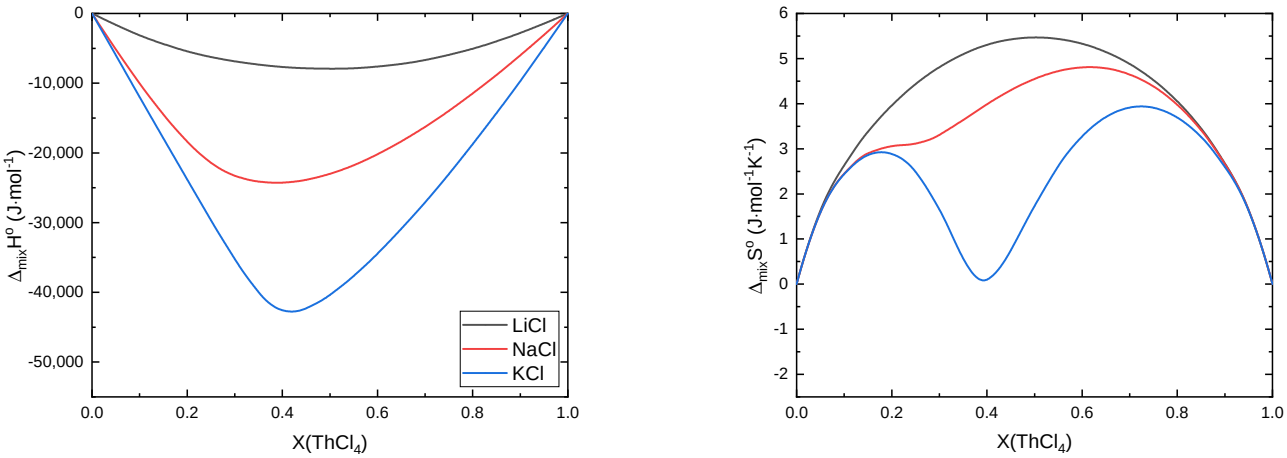

(**a**) (**b**)

Figure 4. (**a**) Enthalpies and (**b**) entropies of mixing of the (A,Th)Cl_x liquid solutions calculated at T = 1100 K.

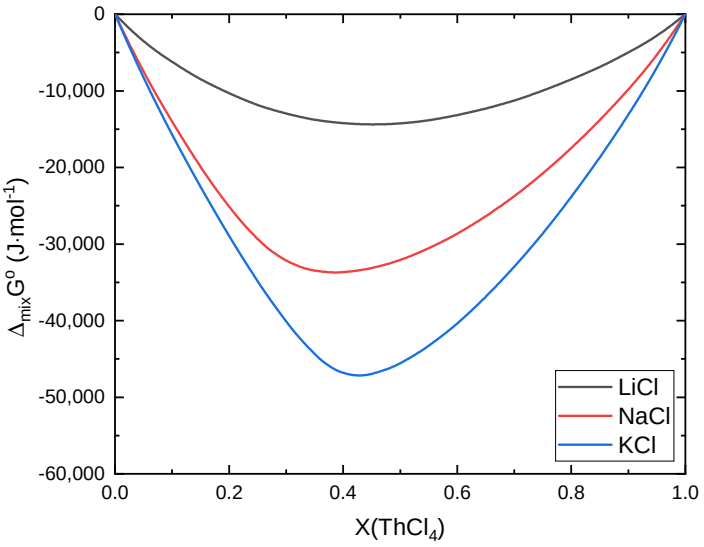

Figure 5. Gibbs energies of mixing of the (A,Th)Cl_x liquid solutions calculated at T = 1100 K.

4. Conclusions

The ACl-$ThCl_4$ (A = Li, Na, K) systems are of metallurgical and nuclear importance. CALPHAD models have been parametrised for them, with a view to assess whether further research on these binary systems is required. The models describe the experimental phase diagrams with a good accuracy. The enthalpies of mixing substantially contribute to the thermodynamic stability of the melts, which increases in the order Li < Na < K. Strong short-range order is apparent in the calculated mixing entropy curves, which become less favourable with the increasing size of the alkali cation: (K,Th)Cl_x even displays an entropy of mixing close to zero where the enthalpy of mixing is greatest in magnitude. The trends in the mixing properties are consistent with simple Coulombic and structural considerations of these salts in the molten state. Still, novel data on these systems are required to better ascertain their phase diagrams and thermodynamic data. Relatively easy access to β-$ThCl_4$ from a reaction between widely available ThO_2 and $AlCl_3$, has recently been described by Deubner et al. [59]. This provides an opportunity to, among other things:

- Isolate the intermediate phases Li_4ThCl_8, Na_2ThCl_6, and $KThCl_5$ and elucidate their crystal structures;
- Derive their standard enthalpies of formation and standard entropies;
- Obtain novel phase equilibrium data with calorimetry, particularly for the KCl-$ThCl_4$ system;
- Measure enthalpies of mixing for the liquid solutions.

Author Contributions: J.A.O.F.: Conceptualisation, Methodology, Investigation, Formal analysis, Visualisation, Data Curation, Supervision, Writing—Original Draft preparation B.A.S.R.: Investigation R.J.M.K.: Supervision, Conceptualisation, Writing—Review and Editing A.L.S.: Conceptualisation, Methodology, Supervision, Resources, Project Administration, Writing—Review and Editing. All authors have read and agreed to the published version of the manuscript.

Funding: J.A. Ocádiz Flores gratefully acknowledges CONACYT-SENER for financial support.

Conflicts of Interest: The authors declare no conflicts of interest.

References

1. Martin, R. *Superfuel: Thorium, the Green Energy Source for the Future*; St. Martin's Press: New York, NY, USA, 2012.
2. Haas, D.; Hugon, M.; Verwerft, M. Overview of European Experience with Thorium Fuels. In *Nuclear Back-End and Transmutation Technology for Waste Disposal*; Springer: Tokyo, Japan, 2015; p. 197.
3. Beaver, W.; Wikle, K. Powder Metallurgy of Thorium. In Proceedings of the Powder Metallurgy in Nuclear Engineering: The Conference on Powder Metallury in Atomic Energy, Philadelphia, PA, USA, 1 January 1958; p. 82.
4. Hombourger, B. Thermochemical Investigation of Molten Fluoride Salts for Generation IV Nuclear Applications—An Equilibrium Exercise. Ph.D. Thesis, Swiss Federal Institute of Technology Lausanne (EPFL), Lausanne, Switzerland, 2018.
5. Rand, M.; Fuger, J.; Grenthe, I.; Neck, V.; Rai, D. *Chemical Thermodynamics of Thorium*; OECD Nuclear Energy Agency: Paris, France, 2008.
6. Mooney, R. The crystal structure of $ThCl_4$ and UCl_4. *Acta Crystallogr.* **1949**, *2*, 189–191. [CrossRef]
7. Elson, R.; Fried, S.; Sellers, P.; Zachariasen, W. The tetravalent and pentavalent states of Protactinium. *J. Am. Chem. Soc.* **1950**, *72*, 5791–5791. [CrossRef]
8. Sellers, P.; Fried, S.; Elson, R.; Zachariasen, W. The Preparation of Some Protactinium Compounds and the Metal1. *J. Am. Chem. Soc.* **1954**, *76*, 5935–5938. [CrossRef]
9. Mucker, K.; Smith, G.; Johnson, Q.; Elson, R. Refinement of the crystal structure of $ThCl_4$. *Acta Crystallogr. Sect. B Struct. Crystallogr. Cryst. Chem.* **1969**, *25*, 2362–2365. [CrossRef]
10. Brown, D.; Hall, T.; Moseley, P. Structural parameters and unit cell dimensions for the tetragonal actinide tetrachlorides (Th, Pa, U, and Np) and tetrabromides (Th and Pa). *J. Chem. Soc. Dalton Trans.* **1973**, *6*, 686–691. [CrossRef]
11. Schleid, T.; Meyer, G.; Morss, L. Facile synthesis of UCl_4 and $ThCl_4$, metallothermic reductions of UCl_4 with alkali metals and crystal structure refinements of UCl_3, UCl_4 and Cs_2UCl_6. *J. Less Common Met.* **1987**, *132*, 69–77. [CrossRef]
12. Mason, J.; Jha, M.; Chiotti, P. Crystal structures of $ThCl_4$ polymorphs. *J. Less Common Met.* **1974**, *34*, 143–151. [CrossRef]
13. Eyring, L.; Westrum, E.F., Jr. The Heat of Formation of Thorium Tetrachloride. *J. Am. Chem. Soc.* **1950**, *72*, 5555–5556. [CrossRef]
14. Fuger, J.; Brown, D. Thermodynamics of the actinide elements. Part IV. Heats and free energies of formation of the tetrachlorides, tetrabromides, and tetraiodides of thorium, uranium, and neptunium. *J. Chem. Soc. Dalton Trans.* **1973**, *4*, 428–434. [CrossRef]
15. Smith, B.; Thakur, L.; Wassef, M. *Thermochemical Studies of Thorium (IV) and Uranium (IV) Chlorides*; Technical Report; London University: London, UK, 1969.
16. Konings, R. The heat capacity and entropy of actinide (IV) compounds. *J. Chem. Thermodyn.* **2004**, *36*, 121–126. [CrossRef]
17. *Atomic Energy Review, Special Issue No. 5 Thorium: Physic-Chemical Properties of Its Compounds and Alloys*; Atomic Energy Review, Special Issue; International Atomic Energy Agency: Vienna, Austria, 1975.
18. Hubert, S.; Delamoye, P.; Lefrant, S.; Lepostollec, M.; Hussonnois, M. Observation of a phase transition in ThBr4 and $ThCl_4$ single crystals by far-infrared and Raman spectroscopy study. *J. Solid State Chem.* **1981**, *36*, 36–44. [CrossRef]
19. Oyamada, R. Phase Diagrams of $ThCl_4$ Systems Containing NaCl, KCl and LiCl and the Limitation of the Congruently Melting Compounds Formation. *Denki Kagaku Oyobi Kogyo Butsuri Kagaku* **1971**, *39*, 2–5. [CrossRef]
20. Vokhmyakov, A.; Desyatnik, V.; Kurbatov, N. Interaction of thorium tetrachloride with chlorides of the alkali metals. *Sov. At. Energy Engl. Transl.* **1973**, *35*, 1122–1123. [CrossRef]
21. Tanii, S. Phase Diagrams of the systems Thorium Chloride-Alkali Chlorides and Thorium Chloride-Alkali Chlorides. *Denki Kagaku Oyobi Kogyo Butsuri Kagaku* **1964**, *32*, 167–170.
22. Edelstein, N.; Katz, J.; Fuger, J.; Morss, L. *The Chemistry of the Actinide and Transactinide Elements*; Springer: Dordrecht, The Netherlands, 2011.
23. Vdovenko, V.; Gershanovich, A.; Suglobova, I. Thermal and X-ray diffraction studies of thorium chloride-lithium chloride and thorium chloride-sodium chloride binary systems. *Radiokhimiya* **1974**, *166*, 886–889.

24. Gershanovich, A.; Suglobova, I. Thermographic and X-ray diffraction studies of binary systems formed by thorium tetrachloride with potassium, rubidium, and cesium chlorides. *Radiokhimiya* **1980**, *22*, 265–270.
25. Bale, C.W.; Chartrand, P.; Degterov, S.; Eriksson, G.; Hack, K.; Mahfoud, R.B.; Melançon, J.; Pelton, A.; Petersen, S. FactSage thermochemical software and databases. *Calphad* **2002**, *26*, 189–228. [CrossRef]
26. Leitner, J.; Voňka, P.; Sedmidubský, D.; Svoboda, P. Application of Neumann–Kopp rule for the estimation of heat capacity of mixed oxides. *Thermochim. Acta* **2010**, *497*, 7–13. [CrossRef]
27. *SGPS-SGTE Pure Substances Database (v13.1)*. Accessed via FactSage (Version 7.2); Scientific Group Thermodata Europe: Saint-Martin-d'Hères, France, updated 2018.
28. Glushko, V.; Gurvich, L.V.; Weitz, V.; Medvedev, V.; Hachkuruzov, G.; Jungmann, V.; Bergman, G.; Baibuz, V.; Yorish, V. *The IVTAN Data Bank on the Thermodynamic Properties of Individual Substances*; *Chemical Thermodynamics of Thorium*; Nauka Publishing House: Moscow, Russia, 1978.
29. van Oudenaren, G.; Ocádiz-Flores, J. Coupled structural modelling of the molten salt system NaCl-UCl_3. *J. Mol. Liq.* **2021**, Submitted.
30. Plato, W. Erstarrungserscheinungen an anorganischen Salzen und Salzgemischen. I. *Z. Für Phys. Chem.* **1906**, *55*, 721–737. [CrossRef]
31. Pyashyenko, B. Unknown. *Metallurgiya* **1935**, *10*, 85.
32. Murgulescu, I. Heat Capacities in Molten Alkaline Halides. *Rev. Roum. Chim.* **1977**, *22*, 683–689.
33. Dawson, R.; Brackett, E.; Brackett, T. A high temperature calorimeter; the enthalpies of α-aluminum oxide and sodium chloride. *J. Phys. Chem.* **1963**, *67*, 1669–1671. [CrossRef]
34. Capelli, E.; Konings, R. Halides of the Actinides and Fission Products Relevant for Molten Salt Reactors. In *Comprehensive Nuclear Materials*; Elsevier: Amsterdam, The Netherlands, 2020.
35. Chiotti, P.; Gartner, G.; Stevens, E.; Saito, Y. Heats of Fusion and Transformation for Some Metals and Compounds. *J. Chem. Eng. Data* **1966**, *11*, 571–574. [CrossRef]
36. Pelton, A.D.; Degterov, S.A.; Eriksson, G.; Robelin, C.; Dessureault, Y. The modified quasichemical model I—Binary solutions. *Metall. Mater. Trans. B* **2000**, *31*, 651–659. [CrossRef]
37. Beneš, O. Thermodynamics of Molten Salts for Nuclear Applications. Ph.D. Thesis, Institute of Chemical Technology, Prague, Czech Republic, 2008.
38. Capelli, E. Thermodynamic Characterization of Salt Components for Molten Salt Reactor Fuel. Ph.D. Thesis, Delft University of Technology, Delft, The Netherlands, 2016.
39. Ard, J.; Johnson, K.; Christian, M.; Yingling, J.; Besmann, T.M.; Mcmurray, J.W.; Peng, J. *FY20 Status Report on the Molten Salt Thermodynamic Database (MSTDB) Development*; Technical Report; Oak Ridge National Lab. (ORNL): Oak Ridge, TN, USA, 2020.
40. Smith, A.; Capelli, E.; Konings, R.; Gheribi, A. A new approach for coupled modelling of the structural and thermo-physical properties of molten salts. Case of a polymeric liquid LiF-BeF_2. *J. Mol. Liq.* **2020**, *299*, 112165. [CrossRef]
41. Robelin, C.; Chartrand, P. Thermodynamic evaluation and optimization of the (NaF+AlF_3+CaF_2+BeF_2+Al2O3+BeO) system. *J. Chem. Thermodyn.* **2013**, *57*, 387–403. [CrossRef]
42. Thoma, R. *Phase Diagrams of Nuclear Reactor Materials*; Oak Ridge National Laboratory: Oak Ridge, TN, USA, 1959; Volume 2548.
43. Bendall, P.; Fitch, A.; Fender, B. The structure of Na_2UCl_6 and Li_2UCl_6 from multiphase powder neutron profile refinement. *J. Appl. Crystallogr.* **1983**, *16*, 164–170. [CrossRef]
44. Kraus, C. *Phase Diagram of Some Complex Salts of Uranium with Halides of the Alkali and Alkaline Earth Metals*; Technical Report; Naval Research Laboratory: Washington, DC, USA, 1943.
45. Kuroda, T.; Suzuki, T. The Equilibrium State Diagrams of UCl_4-NaCl, UCl_4-KCl, UCl_4-$CaCl_2$ and UCl_4-$BaCl_2$ Systems. *J. Electrochem. Soc. Jpn.* **1958**, *26*, E140–E141. [CrossRef]
46. Blander, M. Thermodynamic properties of molten salt solutions. In *Molten Salt Chemistry*; Springer Netherlands: Dordrecht, Netherlands, 1987; pp. 17–62.
47. Liu, J.; Chen, X.; Lu, J.; Cui, H.; Li, J. Polarizable force field parameterization and theoretical simulations of $ThCl_4$–LiCl molten salts. *J. Comput. Chem.* **2018**, *39*, 2432–2438. [CrossRef]
48. Shannon, R. Revised effective ionic radii and systematic studies of interatomic distances in halides and chalcogenides. *Acta Crystallogr. A* **1976**, *32*, 751–767. [CrossRef]
49. Danek, V. *Physico-Chemical Analysis of Molten Electrolytes*; Elsevier: Amsterdam, The Netherlands, 2006.
50. Papatheodorou, G.; Kleppa, O. Enthalpies of mixing of liquid nickel (II) chloride-alkali chloride mixtures at 810 C. *J. Inorg. Nucl. Chem.* **1970**, *32*, 889–900. [CrossRef]
51. Papatheodorou, G.; Kleppa, O. Enthalpies of mixing in the liquid mixtures of the alkali chlorides with $MnCl_2$, $FeCl_2$ and $CoCl_2$. *J. Inorg. Nucl. Chem.* **1971**, *33*, 1249–1278. [CrossRef]
52. Kleppa, O.; Papatheodorou, G. Enthalpies of mixing of binary liquid mixtures of cadmium chloride with cesium and lithium chlorides. *Inorg. Chem.* **1971**, *10*, 872–873. [CrossRef]
53. Gruen, D.; McBeth, R. Tetrahedral $NiCl_4-$ Ion in Crystals and in Fused Salts. Spectrophotometric Study of Chloro Complexes of Ni (II) in Fused Salts. *J. Phys. Chem.* **1959**, *63*, 393–398. [CrossRef]
54. Smith, G.; Boston, C.; Brynestad, J. Electronic Spectra and Coordination Geometry in Molten Mixtures of CsCl and $NiCl_2$ Containing up to 60 Mole% $NiCl_2$. *J. Chem. Phys.* **1966**, *45*, 829–834. [CrossRef]

55. Photiadis, G.; Papatheodorou, G. Co-ordination of thorium (IV) in molten alkali-metal chlorides and the structure of liquid and glassy thorium (IV) chloride. *J. Chem. Soc. Dalton Trans.* **1999**, *20*, 3541–3548. [CrossRef]
56. Capelli, E.; Beneš, O.; Beilmann, M.; Konings, R.J.M. Thermodynamic investigation of the LiF–ThF_4 system. *J. Chem. Thermodyn.* **2013**, *58*, 110–116. [CrossRef]
57. Manzoor, A.; Pandey, S.; Chakraborty, D.; Phillpot, S.R.; Aidhy, D.S. Entropy contributions to phase stability in binary random solid solutions. *NPJ Comput. Mater.* **2018**, *4*, 1–10. [CrossRef]
58. Forsberg, C.W. Reactors with molten salts: Options and missions. In *Frederick Joliot & Otto Hahn Summer School on Nuclear Reactors, Physics and Fuels Systems*; Cadarache: Saint-Paul-lez-Durance, France, 2004.
59. Deubner, H.; Rudel, S.; Kraus, F. A simple access to pure thorium (IV) halides ($ThCl_4$, ThBr4, and ThI4). *Z. Anorg. Und Allg. Chem.* **2017**, *643*, 2005–2010. [CrossRef]